FEASIBILITY STUDY IN THE APPLICATION OF OPTICAL SIGNAL ANALYSIS TO NON-DESTRUCTIVE TESTING OF COMPLEX STRUCTURES

Prepared under Contract No. NAS1-11749

by

Bill Baker
and
Hugh Brown

AMPEX CORPORATION
Research & Advanced Technology Division
401 Broadway (Mail Stop 3-20)
Redwood City, California 94063

for

NATIONAL AERONAUTICS AND SPACE ADMINISTRATION
Langley Research Center

Prepared by: Bill R Baker
Bill R. Baker
Project Engineer

Approved by:
Bob V. Markevitch
Manager, Signal
Processing Section
Advanced Technology Div.

SUMMARY

Advantages of the large time bandwidth product of optical processing are presented. Experiments were performed to study feasibility of the use of optical spectral analysis for detection of flaws in structural elements excited by random noise. Photographic and electronic methods of comparison of complex spectra were developed. Limitations were explored, and suggestions for further work are offered.

CONTENTS

1.0 INTRODUCTION

The response of a structural element to a given load depends upon the material properties, the boundary conditions, and the geometry of the element. Therefore, it is reasonable to expect that dynamic response would be affected by flaws. In fact, in some contemporary manufacturing plants, defective items are still identified by an experienced inspector who raps the parts with a bar and listens to the ringing.

It is desirable to develop more quantitative methods to evaluate structural elements with the hope that inspection techniques could be simplified or automated. Spectral analysis of the dynamic response is a more technical description of the inspector's role. Of the various methods of spectral analysis, optical techniques offer several advantages.

Optical spectral analysis utilizes a very large data base or time bandwidth product, as described in the Appendix, to produce a Fourier transform of a signal. For many applications in the analysis of communication signals or vibration signals from rotating machines, the optical system provides a large improvement in frequency resolution and signal-to-noise enhancement compared to other methods of Fourier analysis.

This study was undertaken to examine the feasibility of using optical spectral analysis to detect flaws in structural elements. The work was later extended to include development of methods for comparison of complex spectra.

2.0 BACKGROUND OF OPTICAL SPECTRAL ANALYSIS

Many signals appear very complicated when presented as functions of time, but they are easier to understand in terms of spectral content. Fourier transform analyzers provide the frequency description of a signal.

Recently developed optical Fourier transform methods (1) have a very large time bandwidth product, that is, utilize a large data base in the analysis stage. Very high data rates and low cost can also be attained by optical methods, see Cyclops Report (2).

The large TB (time bandwidth product) of optical spectral analyzers offers improved frequency resolution due to the longer time interval T during which a given bandwidth B can be sampled. There is also an enhancement of signal-to-noise ratio because coherent components of the signal are reinforced while random background noise tends to cancel over the longer time interval.

A brief description of optical processing is given in the Appendix, and some examples of spectra are presented in this section.

The spectrum of a signal from an accelerometer mounted on a heavy duty transmission is displayed in 3 modes in Fig. 1. A conventional display of power vs. frequency near 1359 Hz is shown in Fig. 1a. The same frequency interval is included as part of the intensified line in the three dimensional display of Fig. 1c. Arrows also indicate the corresponding segment of the orthographic raster format Fig. 1b.

An indication of the resolution is given by noting that the two peaks of Fig. 1a are separated by only 10.2 Hz while the total band shown on the raster is 2,400 Hz. If a conventional Fourier analyzer with only 500 line resolution were used, it would not be possible to separate the two signals, and some systems would not detect them at all.

The raster format can be considered as a plan view of the isometric display which in turn is composed of conventional power-frequency segments such as the one shown in Fig. 1a. Power is indicated by brightness in the raster display of Fig. 1b. For this example the line rate, explained below, is 37.5 Hz.

A sketch of the coordinate system of the frequency raster is shown in Fig. 2. The line rate F, a reference frequency established at the time of processing, determines the bandwidth of the spectrum. The inclined lines of the raster are frequency loci, line segments on which a bright spot can appear showing that a component at the indicated frequency occurs in the signal being analyzed.

The vertical coordinate is designated coarse frequency because two frequencies lying one above the other on adjacent loci differ by a jump exactly equal to the line rate. On the other hand, two points lying on the same segment have a frequency difference less than the line rate with the difference proportional to the separation.

The origin of the coordinate system corresponds to zero frequency or the DC level. Integral multiples of the line rate lie on loci directly above the origin. Other examples of frequencies include the asterisk at position up one locus above the origin and .4F to the right or at 1.4F. The fundamental,indicated by the circle and the number 1,is up 4 loci and .1F to the right at frequency 4.1F. The next harmonics of that signal are shown by circles at 8.2F, 12.3F, and 16.4F. Squares are used to show the fundamental 3.2F and its first harmonics. In that example, the harmonics "wrap around" from the right side to the left.

The schematic Fig. 2 shows only 20 loci for simplicity, but the usual format used in analysis consists of 64 loci. The schematic was prepared with a computer program which can be used to plot all harmonics of all signals which might be expected to appear in a vibration spectrum. A plot of this type was used to identify most of the signals in the transmission spectrum, Fig. 1, as harmonics of the meshing frequencies of 8 sets of gears.

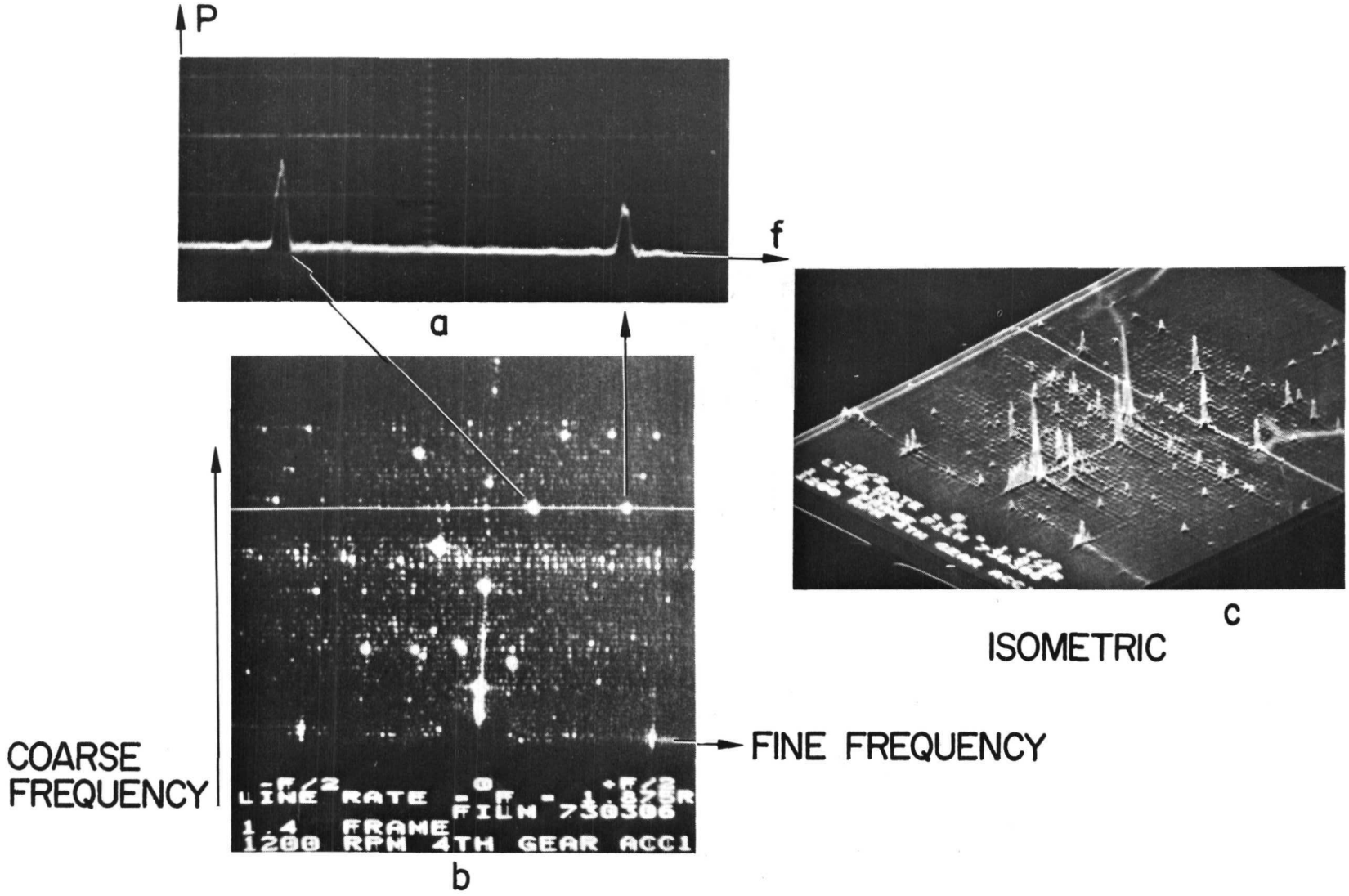

Fig. 1 Spectrum of a Transmission Showing Many Harmonics of Tooth Meshing Frequencies Along With Sideband Signals. Bandwidth 2400 Hz.

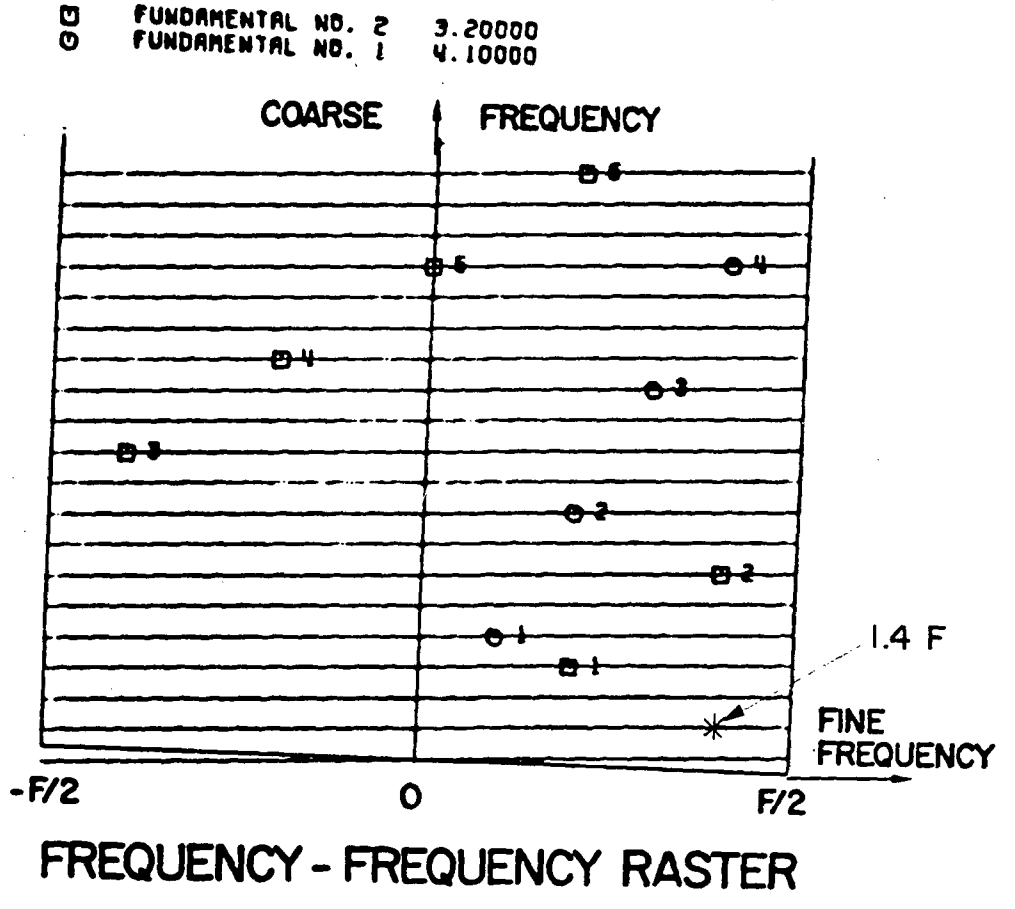

Fig. 2 Raster Frequency Format With Line Rate F

Another example of the extraction of coherent vibration signals from a noisy background is shown in Fig. 3. Vibration spectra from fan and turbine accelerometers of a commercial jet engine are shown with a bandwidth of 3000 Hz. The rear accelerometer spectrum shows strong coherent signals at harmonics of the high speed spool up to the 18th order. These are distinct signals in spite of the presence of a strong noise band at about 600 Hz, possibly caused by the rubbing of turbine seals.

The spectrum of the front accelerometer shows the same harmonics of the rotor plus harmonics of the gear driven accessory power shaft. The noise band at the front accelerometer also is broader and is centered at about 2,000 Hz. Perhaps it is related to rubbing of fan blades.

Experiments have also been run in our laboratories on the spectral changes which occur as the reduction gears of an electric drill were worn. Vibrations were monitored with an accelerometer, and spectra obtained at 4 stages of wear are shown in Fig. 4.

The initial spectrum is somewhat noisy due to newly machined surfaces. After run-in the spectrum is quieter. Additional wear causes sidebands to develop on harmonics of the tooth mesh frequency. The sidebands continued to grow during the life of the gears.

Successful results of optical spectral analysis in the previous applications suggested that the technique might also be used in the detection of structural flaws. Since the resonant frequencies or response of a structure depend upon geometry, it seemed reasonable to try to detect geometrical changes by high resolution spectral analysis.

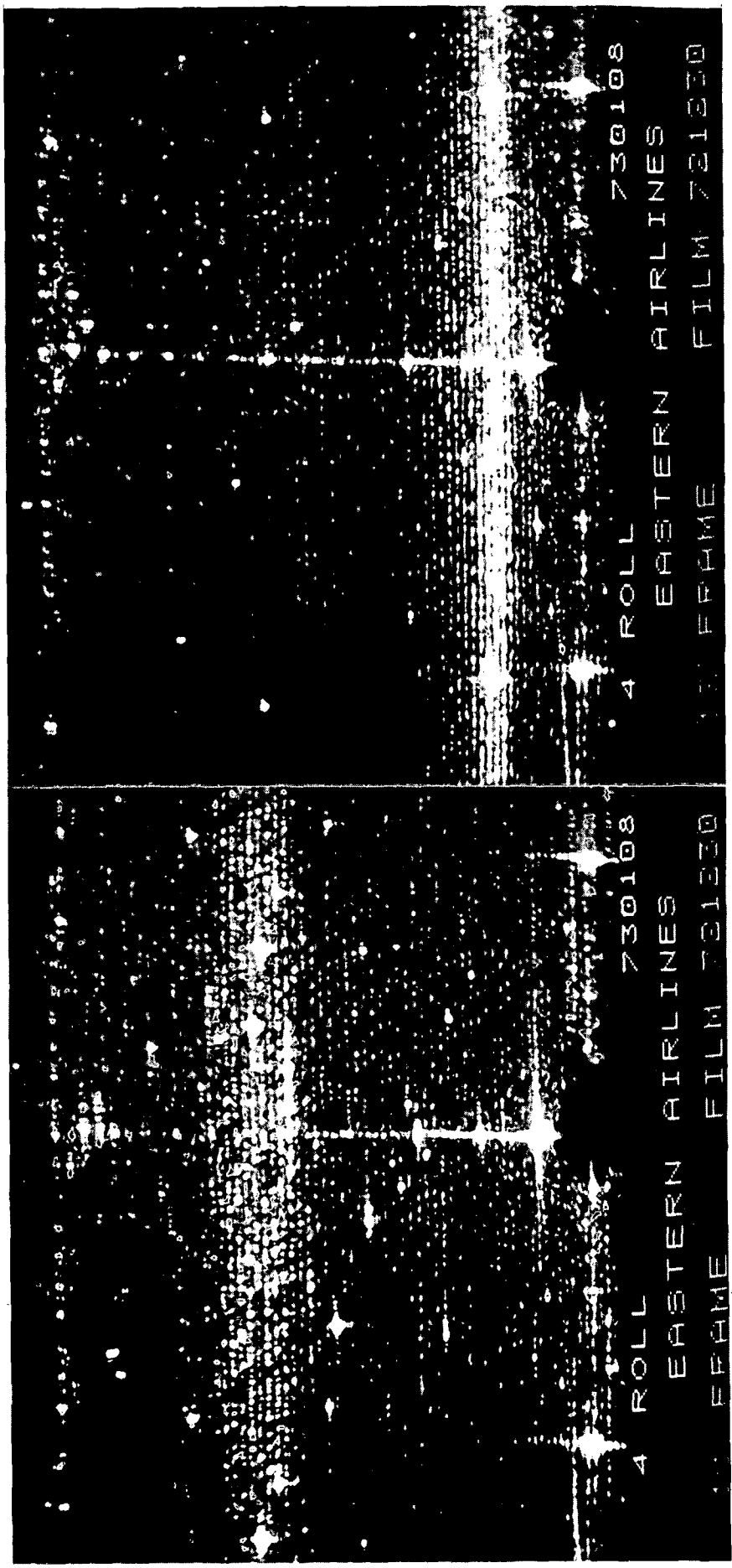

Fig. 3 Spectra From Two Accelerometers on a Jet Engine . Approximate Bandwidth 3000 Hz.

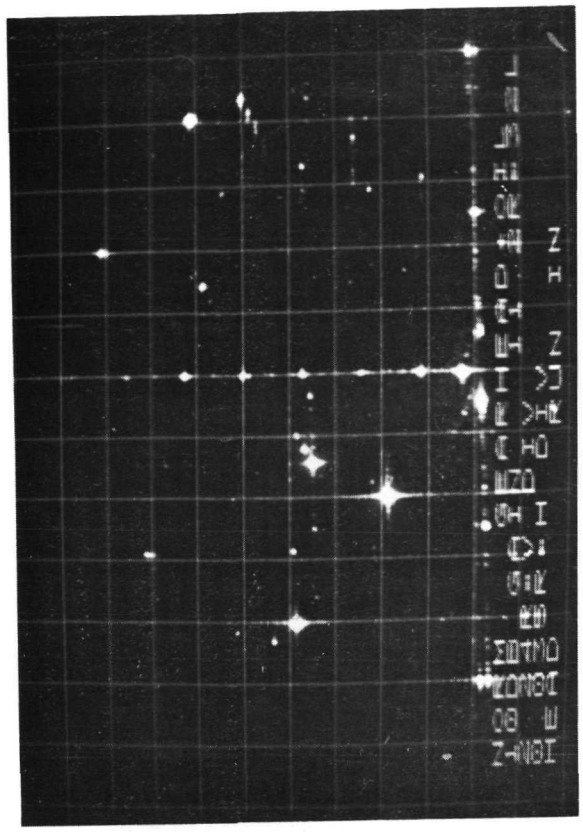

RUN-IN

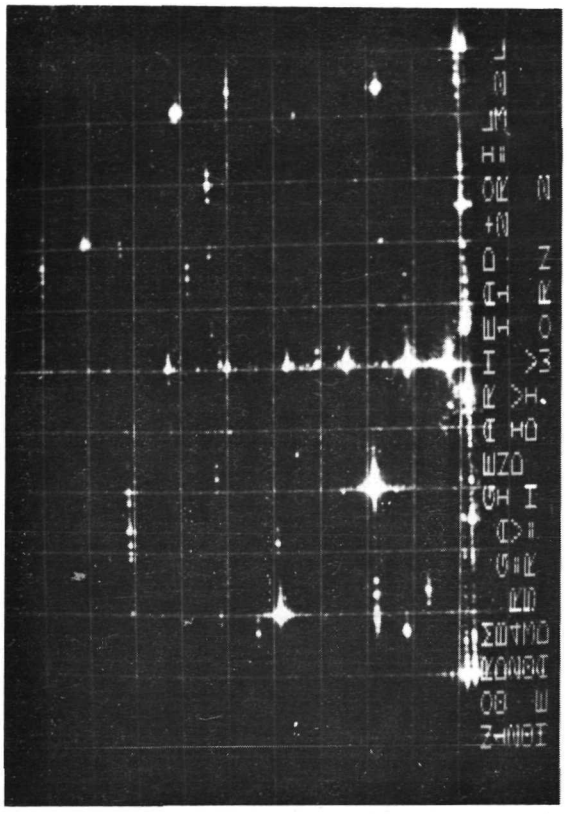

WORN 2

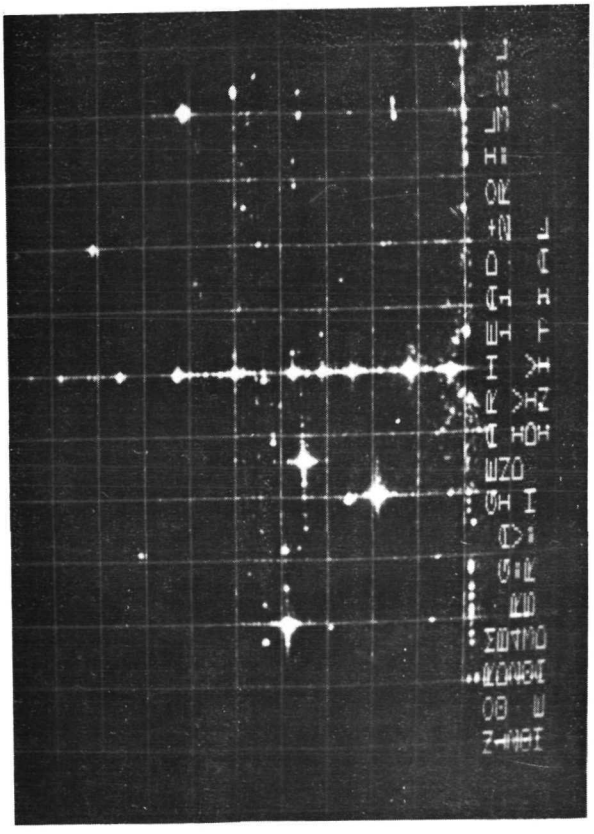

INITIAL

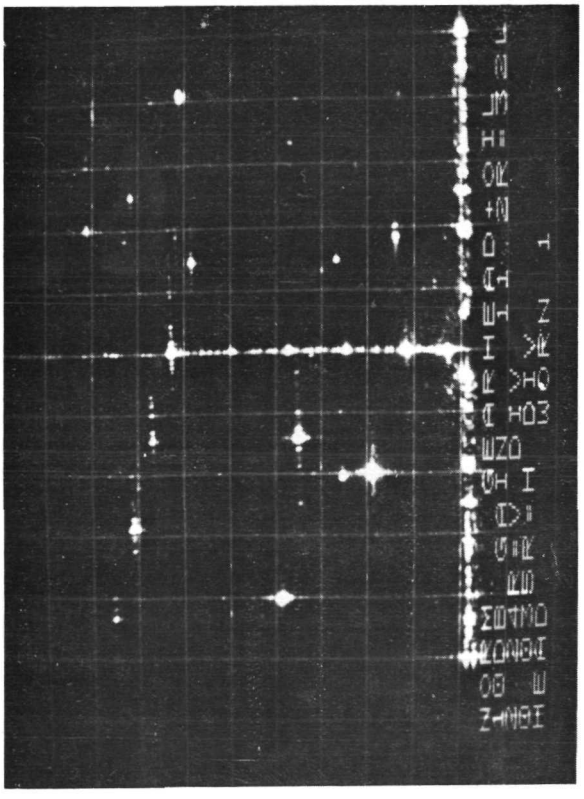

WORN 1

Fig. 4 Comparison of Four Stages in Gear Life

3.0 DYNAMIC RESPONSE OF AN ELASTIC PLATE

3.1 Theoretical Statement of Problem

Propagation of stress waves in an isotropic elastic body can be described in terms of a scalar and a vector displacement field (3). Both portions of the displacement satisfy wave equations in the body. Furthermore, the initial conditions must be fulfilled, and the scalar and vector fields are coupled through stress and displacement conditions on the boundary of the body.

Theoretically the problem is well posed, but, practically, only very simple idealized geometries can be solved. Nevertheless, our understanding of the complicated geometry of the experimental specimens is enhanced by solutions for several of the simpler cases.

3.2 Qualitative Description

For small displacements, the motion can be uncoupled into displacements which are either predominantly along or else transverse to the midplane of the plate. Transverse or bending modes appear to be heavily damped, probably due to greater interaction with the atmosphere. Therefore, transverse motions will be dropped from the discussion.

Because the specimen thickness is very small in comparison with its other dimensions, the propagation through the larger regions of the plate can be described approximately by Lamb waves (4). For very thin plates, such as these specimens, the dominant or high speed Lamb wave is the zeroth order symmetric, S_o, mode with a speed of about 211,600 in./sec. in aluminum.

Simple qualitative descriptions of some modes can be envisioned in which S_o waves are reflected back and forth normal to two parallel edges of the rectangular plate. Of course, interaction with the other plate edges or with holes and transducers complicates the actual process and may lead to reflections over shorter paths. In addition, waves which stike boundaries at an angle will be reflected as a new combination of symmetric and antisymmetric waves. Nevertheless, the simple S_o waves provide an understanding of some frequency components in the spectrum.

Simple surface waves also provide insight into some phenomena which occur at boundaries. For the case of plane motion, waves which travel along the edge of a half space are known as Rayleigh waves (3). The results can also be extended to the case of generalized plane stress (5) which approximately describes the surface waves running along the edge of a thin half plane. The results, see Fig. 5, show that the surface waves traveling on a straight edge of the plate should be no more than 2% slower than the Rayleigh speed.

It has also been shown analytically (6) that the interaction of stress waves with a crack in an unbounded body generates Rayleigh waves which run along the surface and are reflected back and forth between the crack ends. Similar waves also run around the surface of a cylindrical hole in an infinite solid (4).

The preceding examples suggest that surface waves will also race around a hole of any shape in the plate specimen. Furthermore, the wave speed should be only slightly less than 110,500 in./ sec., the speed of Rayleigh waves in aluminum. The frequency at which the waves encircle the cavity is $f = C_s/\ell$ where C_s is the speed and ℓ is the length of the perimeter.

Figure 6 shows the relations between the repetition or resonant frequency for Rayleigh waves running around the circumference of a circular hole or for Lamb waves reflecting back and forth in a bar.

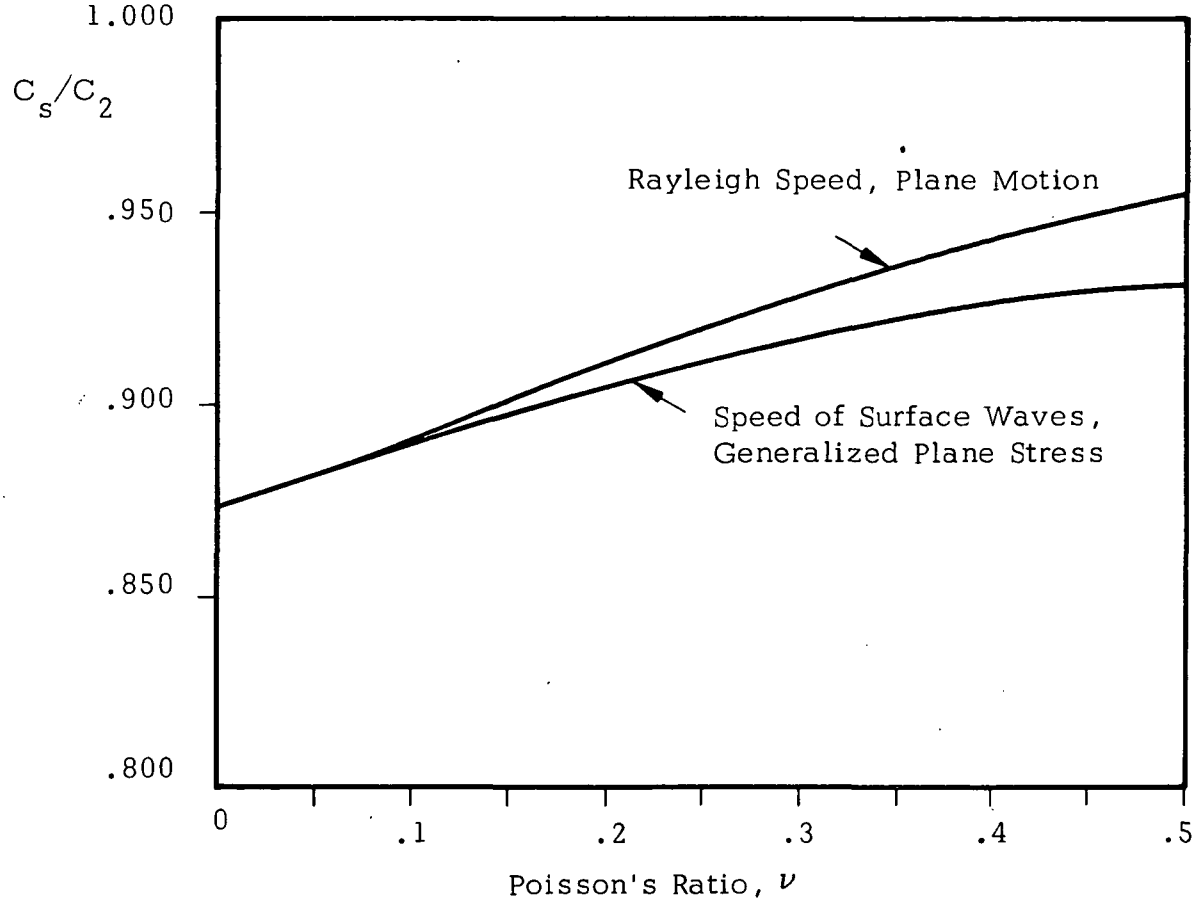

Fig. 5 Speed of Surface Waves on a Half Plane

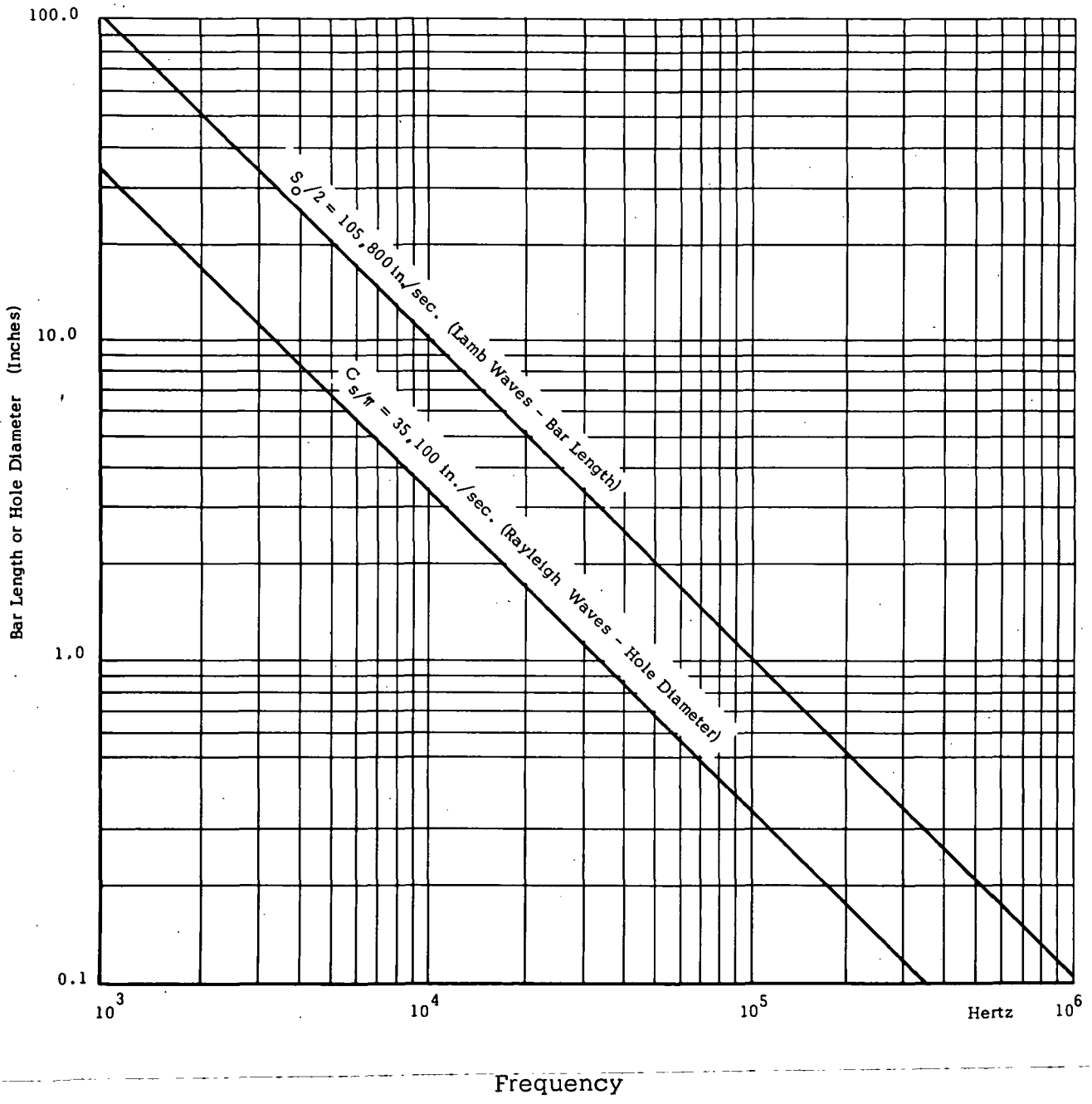

Fig. 6 Repetition frequency for simple waves reflected along a bar or encircling a hole in an aluminum plate.

3.3 Specimen Configuration

All specimens were prepared from .032" (.81 mm) 5052 aluminum. Three basic rectangular shapes were tested with several combinations of holes as simulated flaws. Final experiments were made on 24" (610 mm) square plates as shown in Fig. 7.

It was desired to maintain, as closely as possible, constant edge conditions for different types of flaws. Therefore, initial tests were run with the plate hanging in rubber or nylon slings in order to approximate stress free edges. However, it was soon found that the interesting spectral components correspond to stress waves traveling in the plane of the plate. Therefore, it proved to be adequate to simply lay the plate in a horizontal plane on supports consisting of several blocks of soft styrofoam.

3.4 Transducers

At the start of the program three types of transducers were considered as candidates for pickups. Samples were mounted at corresponding positions on similar specimens for measurements of output signal level.

Two gages of the piezo-resistive type were operated under current supply conditions recommended by the manufacturer for continuous dynamic measurements. The third gage was of the piezo-electric type.

Excitation was provided by a blow from a steel bar at a chosen impact point. Although the applied impulse was controlled only by the operator's sense of motion, it was possible to produce peak output signals within about 20% variation for a given gage. The levels measured on an oscilloscope were of the orders given below:

Table 1 Relative Signals From Three Gages

No.	Transducer Type	Approx. Measured Peak-to-Peak Signal
1	Resistive	.1 mv.
2	P-N Semiconductor	6. mv.
3	Piezoelectric	400 mv.

The output of the resistive gage was so low that noise from the required amplifier nearly obliterated the signal. Preliminary filtering at that stage would improve the signal-to-noise ratio but would, of course, restrict the response in a manner which we wished to avoid. It would be possible to pulse this gage with a higher current level to increase the signal for brief transient measurements, but that approach would complicate the test equipment.

The semiconductor transducer gage puts out a higher signal level, but it has the disadvantage of being a fragile device. The strain sensitive element is sandwiched between a pair of thin glass plates, and the gage must be handled very carefully during mounting.

Because of their higher signal-to-noise ratio and the ruggedness, the piezoelectric transducers were selected as pickups for subsequent experiments. They also have the advantage that they may be used as drivers.

Pickups were prepared from PZT material, .010" (.25 mm) thick and .25" (6.3 mm) square in plan. A circular disc, .50" (12.7 mm) diameter by .016" (.41 mm) thick, of PZT material was used as input transducer. The faces of these materials are silver coated. The Curie temperature is greater than 330°C, so soft solder with a melting point of 220°C could be used to bond the negative face of the PZT slab to a one mil (.025 mm) piece of shim brass used as a ground tab. A lead was attached to the positive face of the slab with a conducting epoxy.

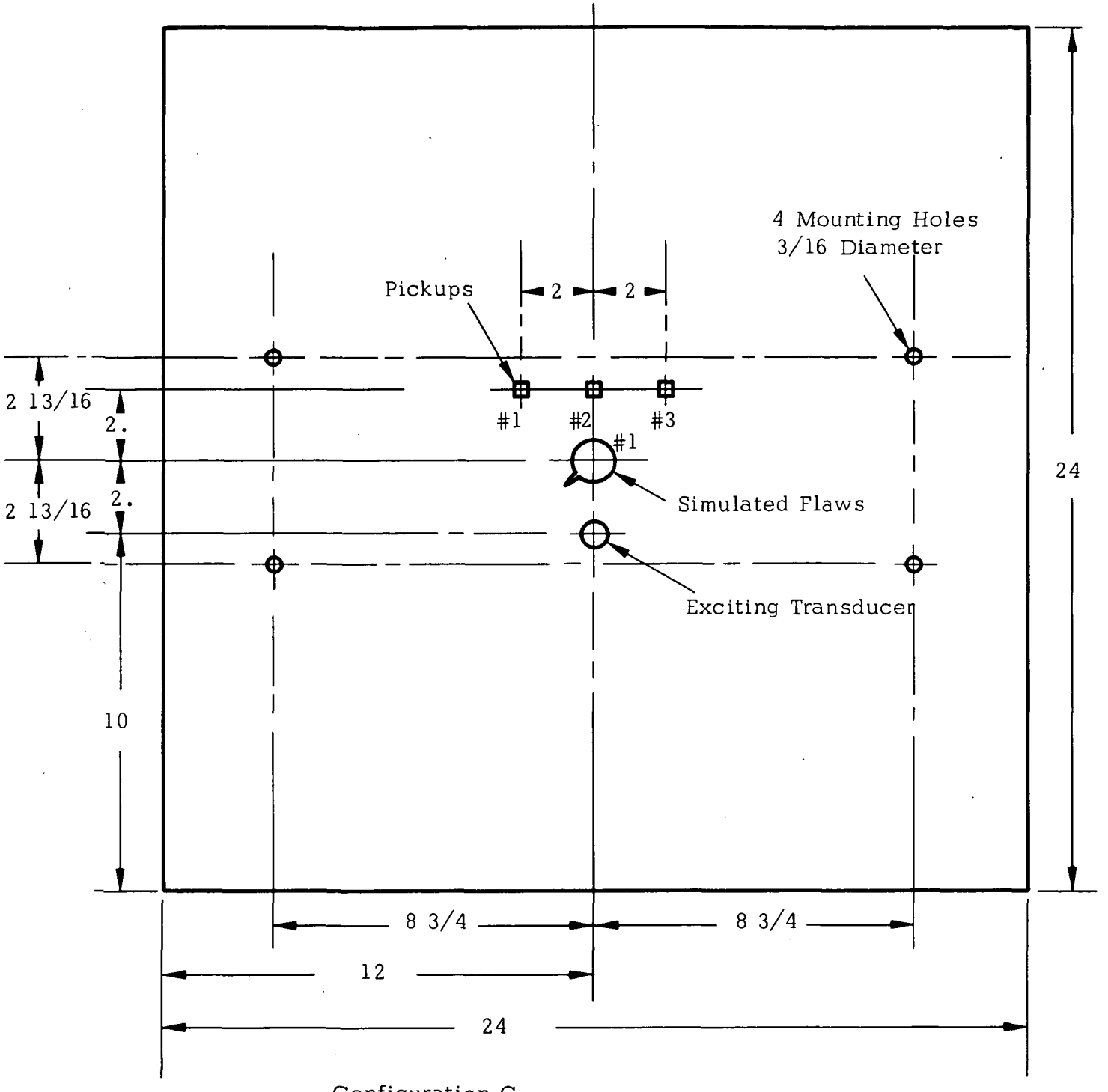

Configuration C

Material 5052 Aluminum
Thickness = .032
All dimensions in inches

Fig. 7 Dimensions of Plate Specimen

The transducers were bonded to the specimen with glycol phthalate which melts at about 140°C. This proved to be an adequate attachment, and it permits repositioning or removal and re-use of the transducers.

3.5 System Response

The plate with associated input and output transducers can be described by a simple linear time invariant model. An input signal $s_i(t)$ produces an output signal $s_o(t)$ according to the convolution integral

$$s_o(t) = \int_{-\infty}^{\infty} h(t-x)\ s_i(x)\ dx$$

where h(t) is the impulse response.

If Fourier transforms are denoted by corresponding upper case letters in the manner

$$S(f) = \int_{-\infty}^{\infty} e^{-j2\pi ft}\, s(t)\ dt$$

then the convolution integral above can be transformed to obtain

$$S_o(f) = H(f)\ S_i(f)$$

The frequency response H (f) or transform of the impulse response can also be described as the output of the system due to unit periodic input $e^{-j2\pi ft}$.

The task is to measure the system response and try to determine variations due to changes in simulated flaws. Any form of input or output could provide a conceivable definition of system response, but the dimensions must be changed if unlike input $s_i(t)$ and output $s_o(t)$ are used.

4.0 RESULTS

Various methods of excitation of the plate were tried and corresponding methods of analysis applied. The general results are described below.

4.1 Pulse Excitation

The simplest method of exciting plate vibrations is to hit the plate with a hammer. In fact, striking the plate edge with a small steel bar was used to evaluate the various types of transducers as discussed in a previous section. However, for our final measurements, it was necessary to use more uniform pulses so a laboratory pulse generator was used to drive a PZT input transducer.

A single pulse proved to be an ineffective stimulus for the plate because the response decayed rapidly due to material and other damping. Because the bandwidth to be examined was approximately 51 kHz and the TB product was 16,000 for the desired display mode, it was possible to sample $16/51 \cong .31$ seconds of data. The vibrations of the plate had dropped down to the noise level in only a few milliseconds so the large TB product of the analyzer was not fully utilized with single pulse excitation.

Some experiments were then carried out with repeated pulses in an attempt to record significant data over a longer time interval. However, the repeated pulses generate an input, and hence output, which is periodic with fundamental equal to the pulse repetition rate and with harmonics depending upon pulse width relative to the period. The simple periodic output appears in the transform as the strength of the output signal at simply related harmonic frequencies.

It was expected that the plate response might be altered in more subtle patterns than could be discerned in these limited samples. Therefore, other sources of excitation were sought.

4.2 Noise Excitation

A search for wider frequency content suggested a random noise generator as source. All frequencies are present at all times but amplitudes vary with time. However, if the sample time is long enough, then the density of the rms value of the signal tends to a value independent of frequency, the white noise distribution.

Tests were run with random noise excitation over the band 0-50 kHz and with the plate containing various simulated flaws. Signals from the three pickups were transformed to obtain output spectra.

Preliminary results of this type, See Fig. 8, showed spectral changes at about 10 kHz and 30 kHz after a 1 inch (25.4 mm) hole had been punched in the plate and after additional notches were cut in the circumference of the hole. Signals with frequency near 10 kHz correspond to vibration modes in which waves are reflected back and forth between the central hole and the plate edges. Surface waves racing around the circumference of the hole have a repetition rate of about 31 kHz.

Early results of this type were encouraging but inconclusive. It was decided to carry out additional experiments to test reproducibility of the results and in particular to determine if the plate could be repeatedly mounted on a simple support with consistent results.

Comparison of spectra by techniques described in later paragraphs revealed that the output was not consistent for an apparently unchanged specimen. The cause was found to be large fluctuations of the average power in a given narrow bandwidth at the input transducer.

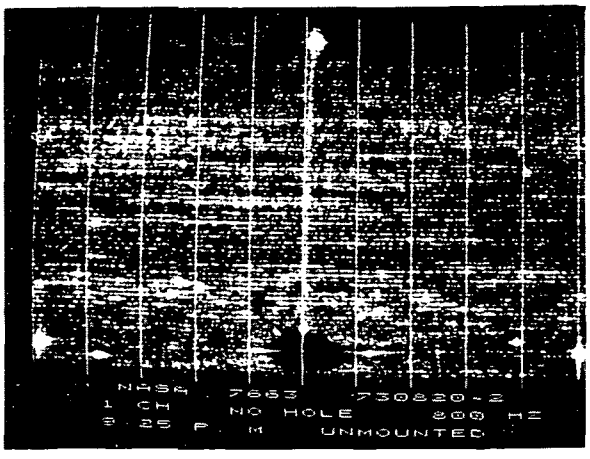

a. No Hole

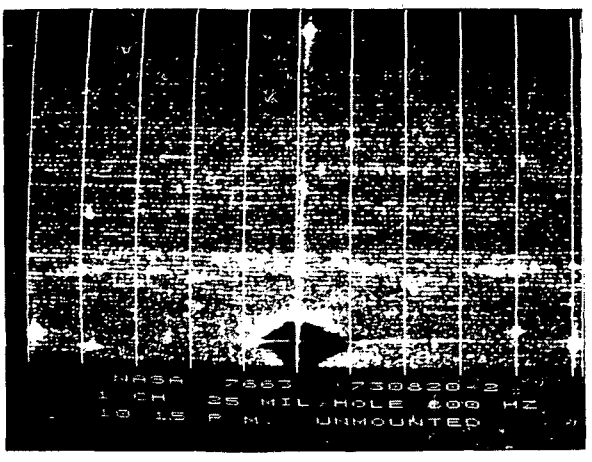

c. Hole With .025" Notch. Decreased Response Near 30 kHz.

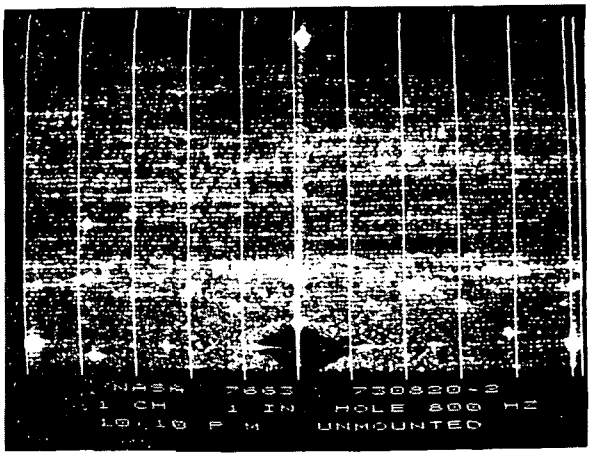

b. One Inch Hole. Changes Near 10 kHz and 30 kHz

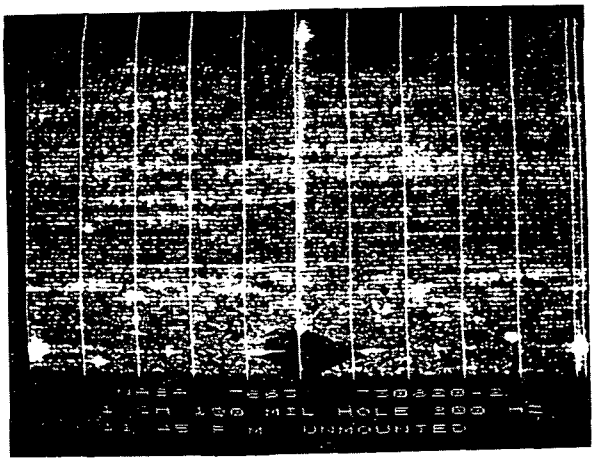

d. Hole With .100" Notch. Additional Changes Near 10 kHz and 30 kHz.

Fig. 8 Spectra of Pickup #1, Random Noise Excitation. Line Rate 800 Hz/Locus, Bandwidth 51,200 Hz

Variations of the output voltage of the noise generator filtered through a 7 Hz passband is shown in Fig. 9. The photograph reveals the shifts in average level taken over a .3 second data acquisition interval corresponding to the 51 kHz bandwidth of the optical analyzer. It can be seen that averages over such brief intervals may change by factors of 2 to 10.

This is an inherent difficulty in trying to use high resolution analysis to identify small scale spectral changes with random noise excitation. Looking for small changes implies studying narrow bands of the spectrum. However, Fig. 9 illustrates the intuitive idea that time averages will vary more significantly for a narrow passband.

Although .3 second appears to be brief it should be remembered than conventional Fourier analysers sample data over a much shorter interval for the 51 kHz bandwidth. Effects of the fluctuations could be reduced by averaging the spectra obtained from several intervals.

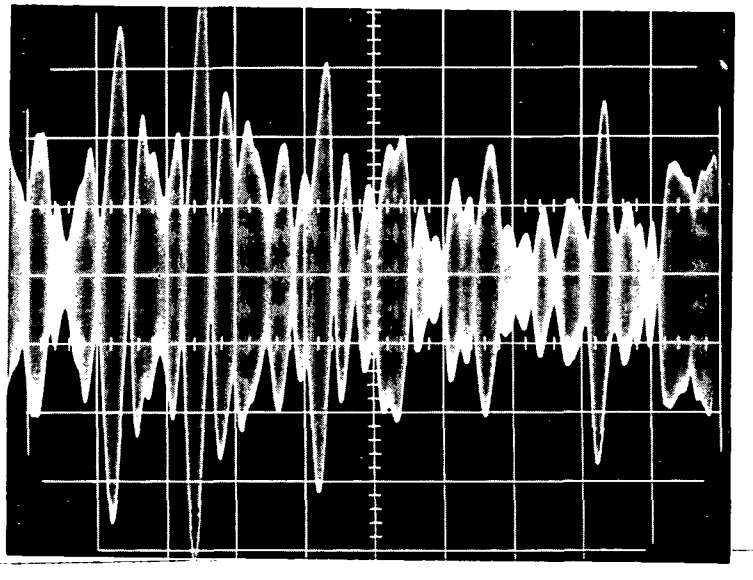

Fig. 9 Relative Output Voltage of Random Noise Generator Filtered Through 7 Hz Passband at 20 kHz. Horizontal Scale: .5 sec/cm.

4.3 Sweep Response

In order to provide a crude estimate of the stability of the plate and transducer system, a series of slow, constant amplitude frequency sweeps were used to drive the input transducer. Two simulated flaws consisting of a one inch hole and either a .10" (2.5 mm) or a .15" (3.8 mm) notch were tested. The plate was alternately tested unmounted and lying on a foam pad or it was mounted with 4 number 8 bolts on a relatively rigid box-shaped card bay.

The square of the response function or output voltage is shown in raster format in Fig. 10. The system for generation of the display is illustrated schematically by Fig. 11. Each point of one of the inclined lines corresponds to a definite time in the 80 second sweep and hence to a definite frequency in the interval 5 kHz to 50 kHz. Sweeps were made in alphabetical order of the photographs.

Comparison of photographs 10c and 10e indicates good reproducibility for the unmounted specimen containing the same flaws. There are noticable differences for the shallower notch of 10a. The cases on the right half of the figure, obtained for the mounted specimen, are not so similar.

4.4 Spectral Comparison Techniques

It was also desired to develop simple methods of comparing spectra. As is described in Appendix A the raster frequency display corresponds to a strip chart 64 times the width of the raster. Comparison of long charts is difficult. It is considerably easier to see changes in the compact raster format, but nevertheless, comparison of two rasters is not trivial.

In order to simplify comparison of spectra, a charge storage tube was used along with the optical processor. The vidicon readout of the spectrum of the response under one set of plate conditions can be stored on the tube . Then a second spectrum from the vidicon can be subtracted from the output of the storage tube to produce a composite represent-

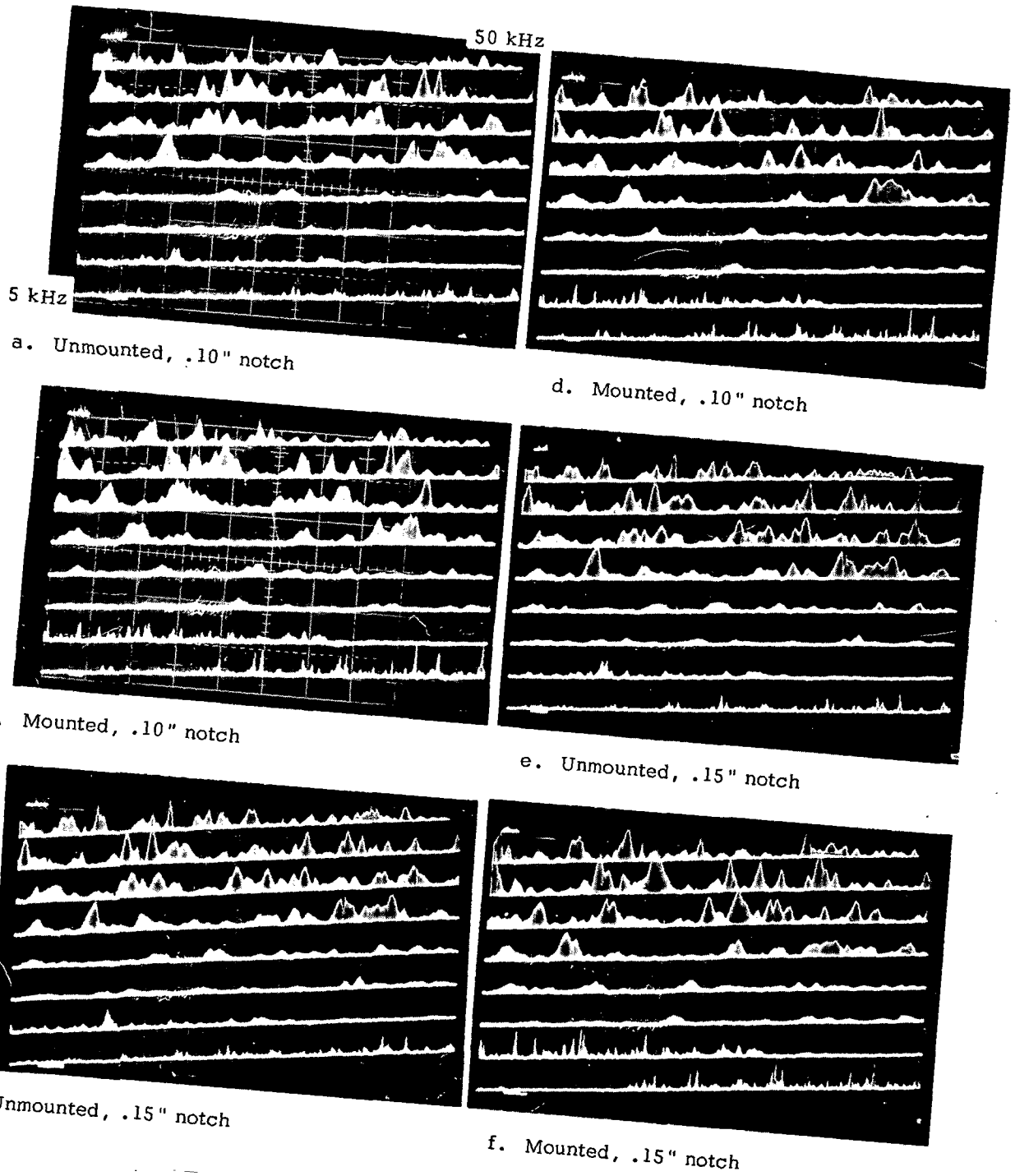

a. Unmounted, .10" notch

d. Mounted, .10" notch

b. Mounted, .10" notch

e. Unmounted, .15" notch

c. Unmounted, .15" notch

f. Mounted, .15" notch

Fig. 10 Response Function or Output Voltage Squared. Frequency Range 5 kHz to 50 kHz Swept in 80 Seconds

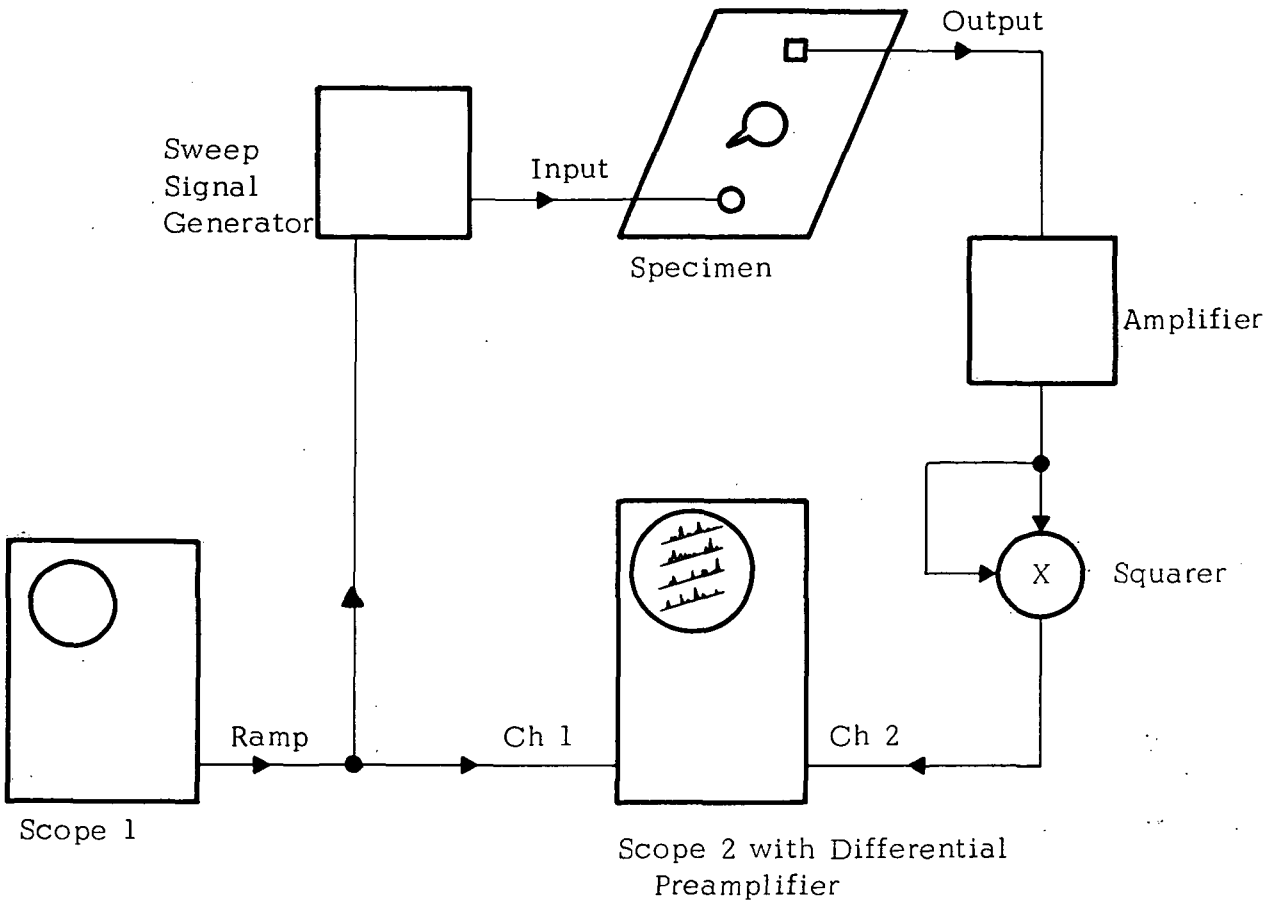

Fig. 11 System for Raster Display of Response

ing the difference of the two spectra. At locations where the spectra show the same amplitude the subtraction leaves an intermediate shade of grey. Presence of a strong component at a given frequency in only one spectrum produces corresponding black or white details.

Initial attempts to compare spectra on the charge storage tube were discouraging. Readout of the stored image produces rotation and translations and a slight scale change with respect to the original video format. Consequently, comparison of a stored spectrum with a second, inverted spectrum being read directly from the vidicon is difficult. Controls have been added to the system to compensate for the geometrical errors, but the process of obtaining good registration is tedious. The correction circuitry should be improved for more convenient operation.

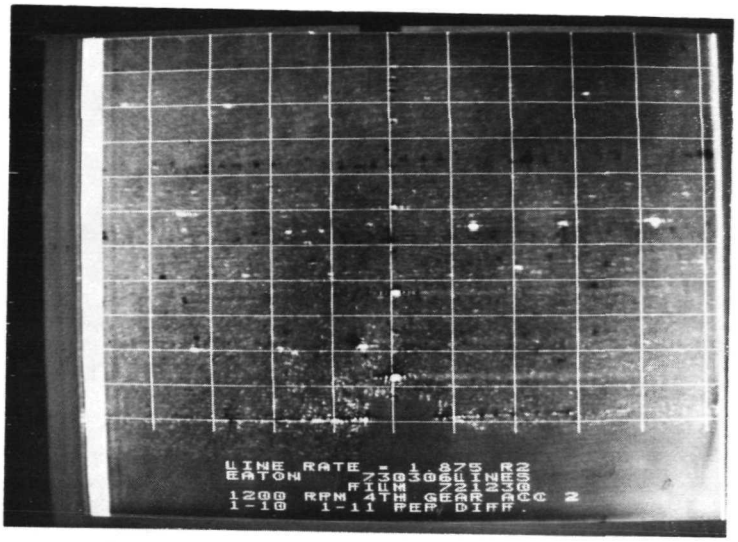

Fig. 12 Comparison of spectra using charge storage tube. Spectrum at 1200 rpm stored positively, strong signals are white. Spectrum at 1500 rpm superposed negatively, strong components appear black.

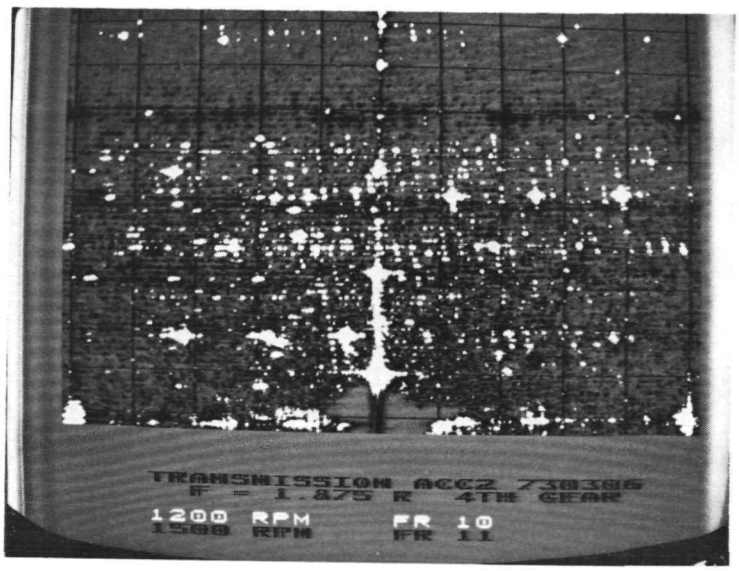

Fig. 13 Comparison of Transmission Spectra at 1200 rpm and 1500 rpm Using Double Exposure on Film and Reversed Polarity Video Signal for Second Spectrum.

5.0 CONCLUSIONS

Optical spectral analysis has been shown to offer high frequency resolution and improved ability to extract a coherent signal from a noisy background. Methods described in this report were not based upon coherent excitation so direct spectral analysis did not provide an opportunity to detect small changes in spectral response due to changes in flaws.

Excitation of the plate by random noise yielded a reasonable description of the response. However, short term fluctuations of the noise generator caused significant variations in the input power spectrum averaged over the finite time of data sampling.

Because of its large data base the optical analyzer tends to average out fluctuations due to the generator. Nevertheless, it appears necessary to average over a longer time interval perhaps by summing several spectra. Further work should include a study of averaging methods.

Double exposure techniques were developed to compare two spectra on a single photographic frame. Partial success was also attained in the use of a charge storage tube for electronic subtraction of spectra. However, the adjustment of the system is tedious and limits routine usage.

Corresponding electronic subtraction could be done using a video disk as storage medium. Preliminary experience in other applications suggested that a disk system is far easier to operate. The simplicity is due to the high state of commercial development and standardization of video disks.

Future work should be based upon signal processing techniques where the large time bandwidth product of optical spectral analysis can be used more fruitfully. These investigations should include consideration of beam scanning methods.

6.0 REFERENCES

1. Goodman, J. W., Introduction to Fourier Optics, McGraw-Hill, New York, 1968.
2. Oliver, Bernard M., Project Cyclops, NASA Rpt. CR 114445, 1971.
3. Sokolnikoff, I.S., Mathematical Theory of Elasticity, McGraw-Hill, New York, 1956.
4. Viktorov, I.A., Rayleigh and Lamb Waves, Plenum, New York, 1967.
5. Baker, B.R., "Tearing of Viscous Fibers," Int. J. Fracture Mech., 1968 and (in Russian) Mekhanika Tverdovo Tela, Proc. Acad. Sci, USSR, 1969.
6. Baker, B.R., "Dynamic Stresses Created by a Moving Crack," Proc. Tenth Int. Cong. Appl. Mech., Stresa, Italy, 1960, and J. Appl. Mech., 1962.
7. Bracewell, Ron., "The Fourier Transform and its Applications, McGraw-Hill, New York, 1965.
8. Carlson, A.B., Communication Systems, McGraw-Hill, New York, 1968.

1.0 FUNDAMENTALS OF OPTICAL PROCESSING

1.1 Introduction

In this chapter, optical processing and the formats of data recording and spectral presentation will be described briefly. Then the theory will be discussed first in an intuitive manner and later in a more mathematical form for a reader who is more familiar with Fourier analysis.

The advantages of optical information processing are its high resolution of frequencies and great enhancement of the signal-to-noise ratio. The latter refers to the ability to extract significant distinct frequencies from extraneous background noise. The capability of any spectral analyzer can be described in terms of its time bandwidth product or the number of data samples which are stored and, later, treated in the process of analysis. For conventional digital or analog analyzers, the number of samples may only be of the order of 10^3 digital words or analog values. On the other hand, the cathode ray tube recorder to be described here stores about 10^5 samples on a square centimeter of film. Other optical recorders developed by Ampex store about 10^6 samples on the same area.

As in all spectral analyzers, the data must be sampled at least two and preferably about three times per cycle of the highest frequency to be analyzed. If that highest frequency, or bandwidth, is denoted by B and if the recording time is T, then the number of samples must be 2BT (or preferably 3BT). Since the storage capacity is fixed, it is possible to trade off bandwidth versus the recording time. It can also be shown that the frequency resolution of the analyzer is the reciprocal of the recording interval, T.

Consequently, the frequency resolution of the optical processor is of the order 10^{-5} to 10^{-6} times the bandwidth.

The system diagram of Fig. 1.1 illustrates the steps in optical processing beginning with the optical recording of a signal and the subsequent optical processing and display of the spectrum. The optical recording is simply a photograph of the face of a CRT which is scanned in a manner similar to that of a TV tube with the intensity of the beam being modulated by the incoming signal.

The film is chemically processed in a few seconds with a Bimat technique and is then ready for spectral analysis in the optical processor shown in the lower portion of Fig. 1.1. The spectrum is focused on the face of a TV camera which is used to produce displays on an orthographic TV screen and on a 3D or isometric screen at the right.

A minicomputer has also been tied into the system to perform certain calculations, to display alphanumeric data on the TV screens and to produce hard copy of special data.

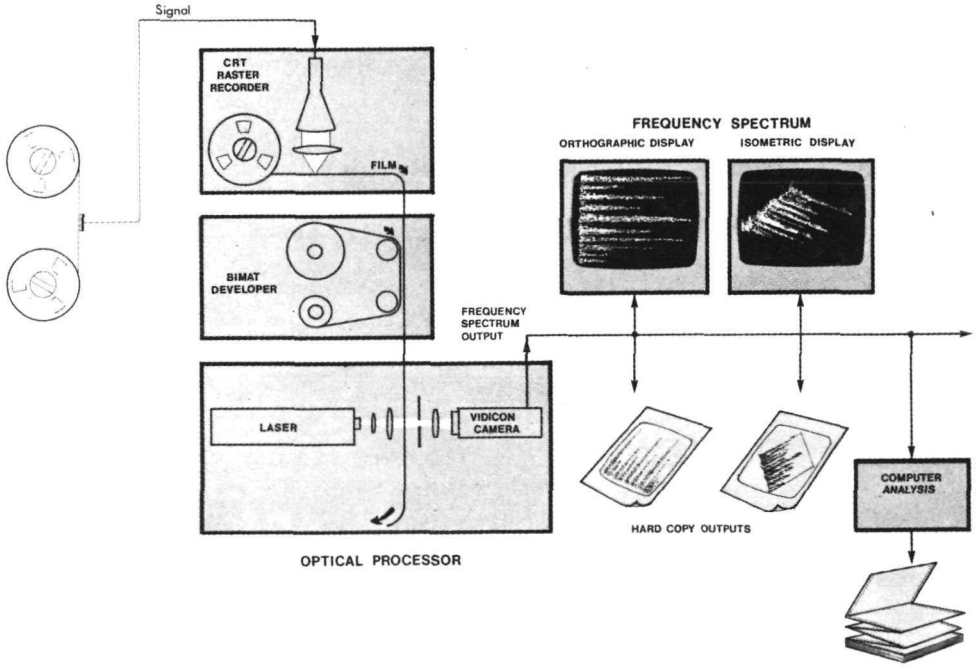

Fig. 1.1 Schematic of Optical Processor

1.2 Optical Recording

The first step of the optical analysis is the transfer of an electrical signal, which may have been temporarily stored on magnetic tape, onto a photographic film. Each data sample is transferred so that a very small spot of the film will be subjected to an exposure proportional to the sampled voltage. After chemical processing the film spot has a transmittance proportional to the voltage of the original sample. Of course, the optical transmittance of the film can never be negative so a uniform bias or DC level must be added to the signal to maintain the transmittance in a positive range. In the CRT recorder the film is exposed by the beam spot on the tube face. The beam intensity is modulated by the sum of the signal and DC bias voltages.

Of the many formats which could be used for placing data samples or spots on film, two examples are illustrated in Fig. 1.2.

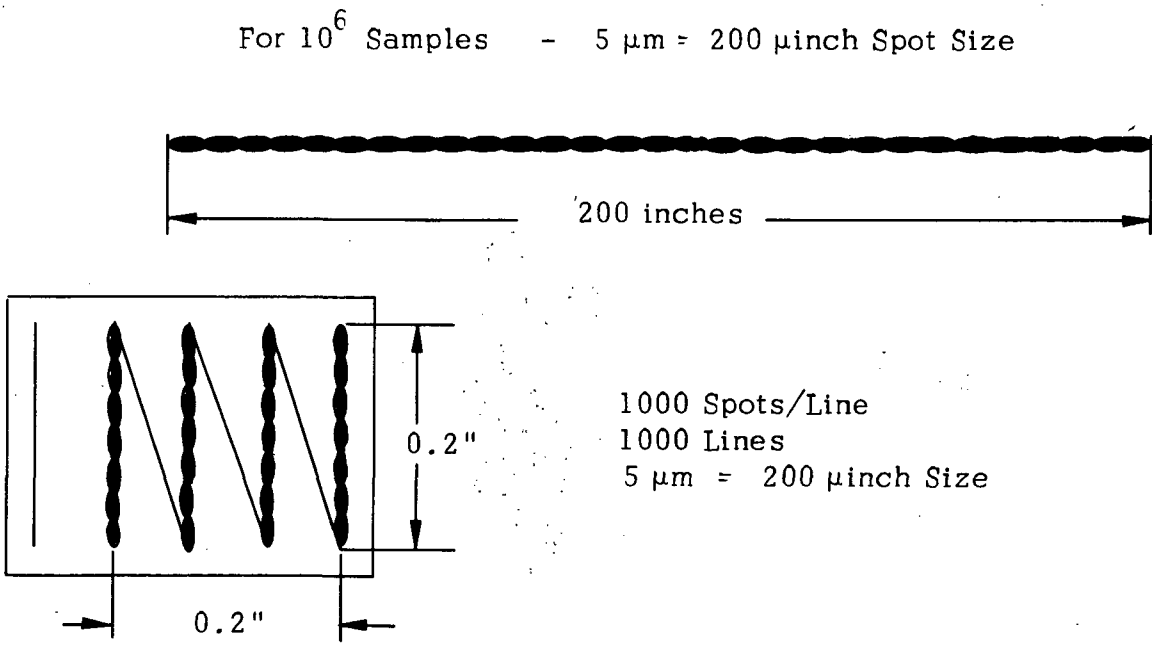

Fig. 1.2 Comparison of Linear and Raster Formats

The sketch at the top shows a million sample spots placed in a straight line. That geometry corresponds to a single track of a consumer tape recorder. Even for a small spot diameter of 2×10^{-4} inch, the film would have to be 200 inches long! Not only would the film be expensive and difficult to handle but the illumination which is required during the processing stage would be impractical for such a long strip.

The second, folded or raster format shows that the same million samples could be stored in a 0.2 inch square. The major advantage of the compact raster format is that the large number of data samples can be uniformly illuminated and analyzed in the processing stage.

To make the raster recording on film, the system sketched in Fig. 1.3 is employed. The camera shutter is opened, and a time exposure is made as the CRT beam scans a single frame on the tube face. The beam is stepped across the scan line from one spot to the next with position corresponding to time. At each spot the beam is stopped, and the intensity is modulated by the value of the data sample. Flyback occurs in negligible time at the end of each scan line.

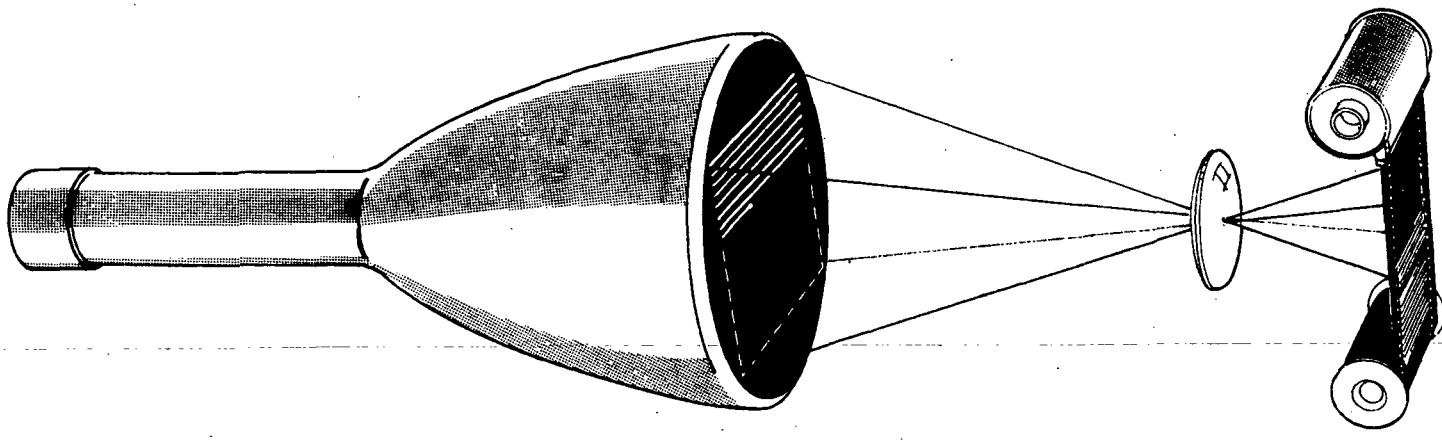

Fig. 1.3 The Raster Scanned on the CRT is Photographed to Produce the Optical Recording

The resulting optical recording is similar to a photograph of a single frame from a TV screen if the intensity were modulated by the data. The recording looks almost like a grating or a set of parallel uniformly spaced lines. However, the transmittance of the lines varies in agreement with the data values at the corresponding time of the recording.

The bandwidth of the recording is established by the choice of line rate, or the time required for the CRT beam to scan one line, and the number of data points per line. As an example, suppose that a line is scanned in 0.1 second; in other words, the line rate is 10 lines per second (10 Hz). Let the number of data points per line be 360. Then according to the sampling theorem the maximum spatial frequency on the film is about 360/3 = 120 cycles per line. This corresponds to a bandwidth of 120 cycles/line times 10 lines/second or 1200 Hz. If the scan time were doubled (0.2 second) then the line rate would be 5 lines/second (5 Hz) and the bandwidth 600 Hz. Decreasing the scan time to .05 second increases the line rate to 20 lines/second (20 Hz) and the bandwidth to 2400 Hz.

1.3 Diffraction and the Frequency Plane

Diffraction by a grating is the fundamental physical phenomenon utilized in spectral analysis of the optical recording. Diffraction is illustrated by Fig. 1.4 where the recording has temporarily been represented by a grating of lines of constant transmittance on the film.

If the grating is illuminated by a coherent monochromatic light source, such as a laser beam, then at great distances diffraction produces bright dots along an axis perpendicular to the lines of the grating. There is a bright spot called the zero order on the line normal to the film plane. The next bright spot, labeled "line rate", corresponds to f_ℓ the spatial frequency of the grating. Since the variation of transmittance of the grating across the lines is not perfectly sinusoidal, there are also bright spots at the harmonics $2f_\ell$, $3f_\ell$, etc., and because of symmetry, there are

corresponding dots at $-f_\ell$, $-2f_\ell$, $-3f_\ell$, etc. in the opposite direction from the zero order. These line rate dots and a few harmonics can even be observed by looking through a grating at a small, distant light bulb in a dark room.

The lens is added so that the transform plane containing the spectrum or harmonic content of the grating can be brought conveniently close to the film plane. Of course, if the grating is rotated in its plane then the harmonic spots in the transform plane rotate through the same angle. Also, if two gratings, perhaps of different pitch, are superposed with a relative rotation then the harmonic spots of each grating will appear with the same relative rotation in the transform plane. Furthermore, the nodes or intersections of the two gratings form a periodic system, a Moiré pattern, which can be considered as points on many different gratings, each of which has a corresponding set of harmonic spots. The result is a set of spots on parallel lines in the transform plane.

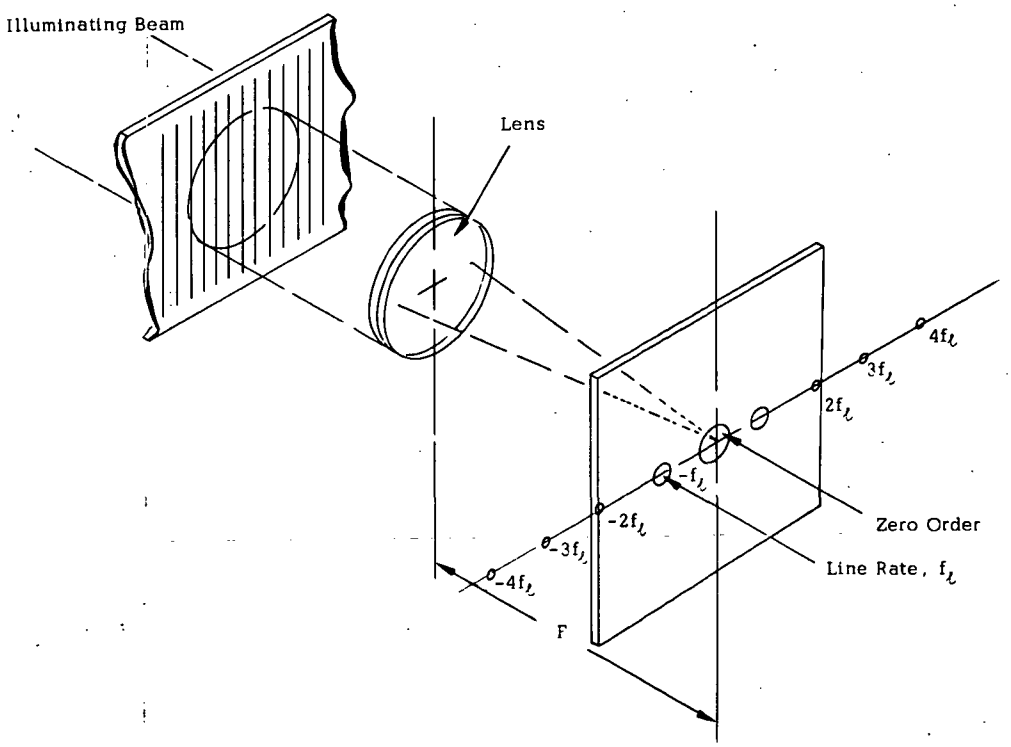

Fig. 1.4 Diffraction Pattern Produced by a Grating of Spatial Frequency f_ℓ

Attached to this page is a strip of 35 mm film with a recorded transverse grating similar to the one illustrated in Fig. 1.4. The line rate dot and harmonics can be observed by looking through the grating at a small distant light source such as the filament of a flashlight bulb. White light from the bulb will be diffracted by an amount depending upon the various wave lengths. The result is smearing of the dots into the color spectrum of the source.

Better definition of the dots is obtained if the bulb is covered by a colored glass or celophane filter to restrict the spectrum to a narrow band of color. The distant, filtered bulb produces nearly monochromatic waves which are almost flat when they strike the grating. A laser produces better quality waves at much higher intensities which makes modern optical processing feasible.

We return now to the optical recording of a single constant wave. As indicated in Fig. 1.5 the basic line structure creates the zero order and line rate spots in the frequency plane. Furthermore, the transmittance of the grating varies sinusoidally at a constant rate along each scan line which leads to other diffraction phenomena.

Figure 1.6 shows how we can also form a Moiré pattern consisting of imaginary lines connecting the peaks of the sine wave and running longitudinally along the film. In the particular example shown here, precisely 12 cycles of the signal have been recorded along each scan line. This pattern will contribute the two solid dots to the transform plane. Had the signal frequency been slightly higher, so that, say, 13 cycles per line had been recorded, then this signal would form dots (broken-line circles in Fig. 1.6), further away from the origin, since distance from the origin is proportional to the spatial frequency in the recording.

We can also develop other sets of Moiré patterns. As shown in Fig. 1.7, the peaks of the recorded sine waves could be connected with other imaginary lines. This new grating will produce the pair of dots in the upper right and lower left quadrants of the transform plane. Another set of lines can also be drawn and will generate the pairs of dots shown by broken-line circles in the upper left and lower right quadrants.

1.4 Interpretation of Frequency Display

More detailed studies of the Moiré structure, or the Fourier description presented in a later section, show that the spectrum or the light distribution in the frequency or transform plane has the basic form indicated in Fig. 1.8. The format is a raster because the original recording was also made in a raster. The reference frequency or line rate of 10 Hz indicates that the original optical recording was made at a rate of 10 lines per second or a scan time of .1 second per line.

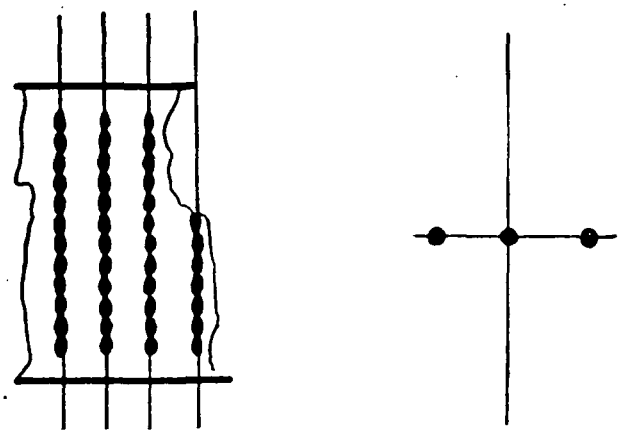

Fig. 1.5 The line grating itself transforms into a d-c term at the origin and a pair of dots whose distance from the origin is determined by the line-to-line spacing.

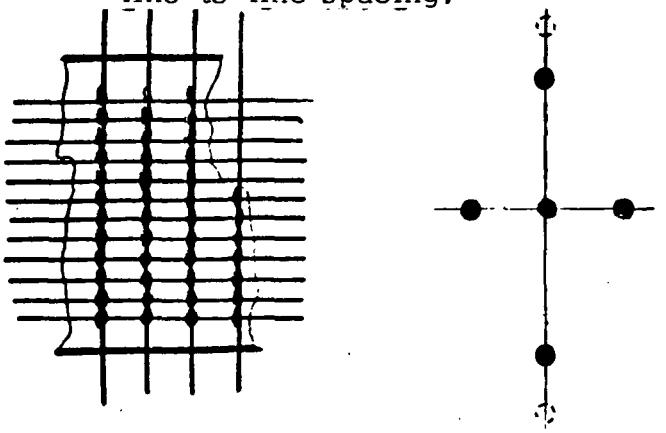

Fig. 1.6 The signal peaks also form a raster. If each raster line carries an integral number of cycles, the signal raster will be transformed into a pair of dots on an axis orthogonal to the line-grating transform.

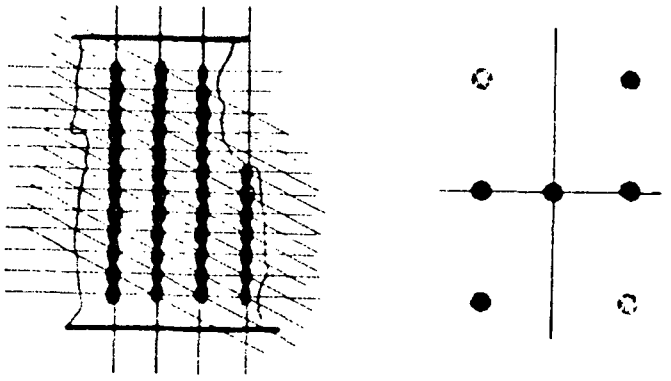

Fig. 1.7 Other peak-to-peak rasters can also be imagined, and transformed into additional dots.

Interpretation of the spectrum can be illustrated by considering a sequence of recordings each of which is made for a constant wave with frequency slightly higher than that of the previous recording. If the first recording is of a DC signal then the optical recording is a grating with constant transmittance along each scan line. The result, as we noted before, is just the zero order spot and the spots at harmonics of the line rate f_ℓ. The zero order spot can be chosen as the point in the frequency plane which represents DC or zero frequency.

Suppose the next recording is made of a constant wave with frequency of 2 Hz. Then the transform plane will still contain the zero order and harmonics of the line rate. However, the spot representing the signal frequency will lie on the lower inclined line, labeled zero locus, in Fig. 1.8, and it will be 2/10 of the distance toward the point above the line rate dot at the right edge of the screen.

If signals of increasing frequency up to 10 Hz are analyzed, the corresponding frequency spot will move to the right along the zero locus. At a signal frequency of exactly 10 Hz , the spot will lie exactly above the line rate dot, and a second spot will appear on the first locus directly above the zero order. An increase in frequency to say 13 Hz will move the spot to a position 3/10 of the distance along the first locus toward the point over the line rate dot.

Further increase of the signal frequency would trace out a series of loci or line segments each representing a frequency interval equal to the line rate. The coordinates in the frequency plane are both measures of frequency. Moving horizontally along a locus corresponds to a continuous change in frequency, but moving upward from one locus to the next corresponds to a frequency jump exactly equal to the line rate.

The position along a locus is called the fine frequency coordinate. It is analogous to the fine time coordinate measured along a scan line in the optical recording. The vertical position in the frequency plane is called the coarse frequency coordinate because vertical motion from one locus to the next corresponds to a frequency jump equal to the line rate. This also resembles the coarse time coordinate in the film plane where a jump from one line to the next corresponds to a time jump equal to the scan interval.

Up to this point, the spots in the transform plane have only been described as indicators of the frequency of a particular signal component. However, the intensity of the spot is also proportional to the power of the original signal.

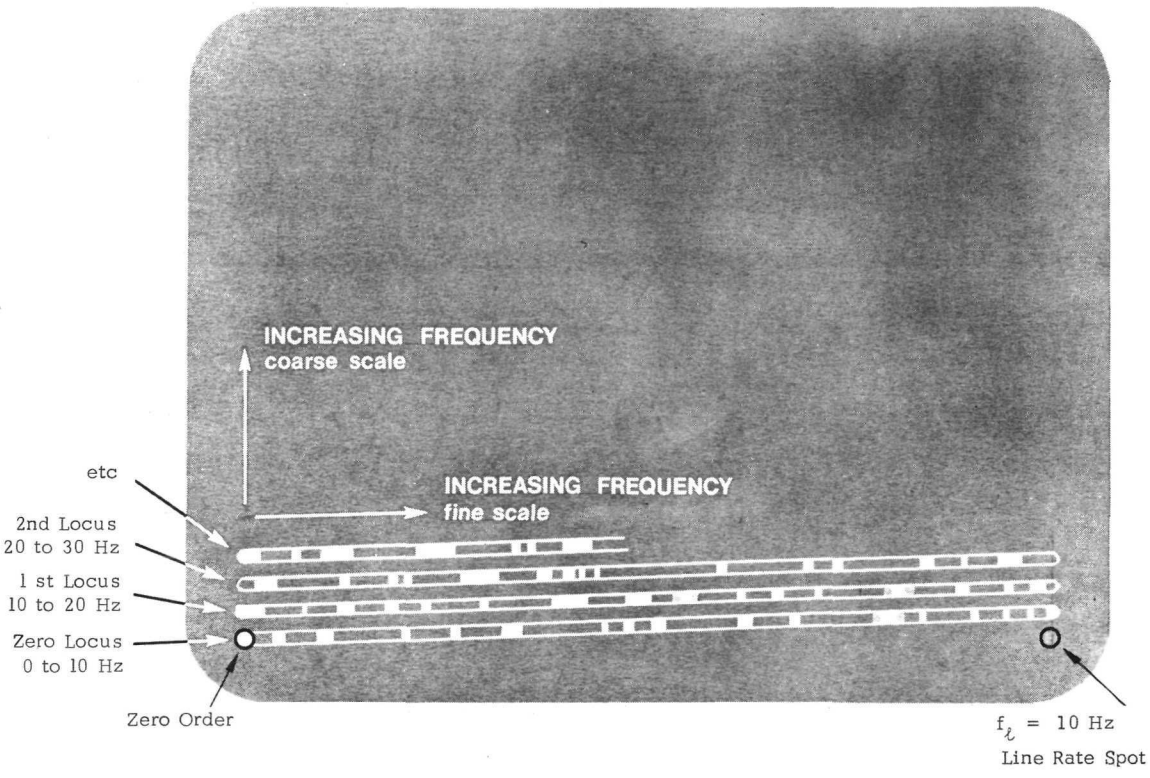

Fig. 1.8 Raster Format of Spectrum. Light Intensity is Proportional to Signal Power.

A more conventional representation of signal power versus frequency is illustrated by the strip chart at the top of Fig. 1.9. That sketch also indicates the correspondence of the first 10 Hz segment of the strip chart with the zero locus of the raster display. The light intensity at a point on the locus is proportional to the signal power at the corresponding frequency.

A little practice makes it easy to interpret brightness in the raster transform plane in terms of the signal power at a given frequency point. Furthermore, the transform shown in Fig. 1.8 may contain segments of 64 or more loci each about 10 inches long on the TV screen. As shown by Fig. 1.9, an equivalent strip chart would contain 64 of the segments and be more than 50 feet long! Therefore, the compact raster format has the additional advantage of helping the user recognize signal patterns and changes much more easily than if he had to view a long strip chart.

For those cases where a more quantitative description of the power spectrum is desired, an isometric display is also provided on a second TV screen. This presentation may be visualized as a 3 dimensional relief map of intensity raised above the frequency base plane of Fig. 1.8. Creation of the relief map from a strip chart provides another interpretation. Each segment of the strip chart corresponding to a locus segment as shown in Fig. 1.9, could be cut along the power trace. Then each "ridge of intensity mountains" would be glued in an upright position over the corresponding locus in the raster frequency plane of Fig. 1.8. The resulting 3 dimensional relief map can be viewed from any angle.

Of course, electronic signals from the TV camera are mixed and displayed on a monitor to form the isometric in the system. Controls are provided to rotate the map about any of its 3 axes and to change scales. The rotation is sometimes useful to provide a better view of details hidden by a tall "mountain" produced by an intense signal.

An example of the spectrum of a reciprocating air compressor is shown in Fig. 1.10. The same spectrum is shown in a three dimensional form in Fig. 1.11.

1.5 Relation to the Fourier Transform

The Fourier transform can be derived from the physics underlying the system sketched in Fig. 1.12. In this example the propagation of light can be described by one scalar wave equation as in the case of acoustics. The propagation between a point source such as P_1 in the film plane and an observation point such as P_o in the frequency plane is governed by the simple exponential form $\exp(-j\,2\pi r_{01}/\lambda)/r_{01}$. Here r_{01} is the distance between source and observation points and λ is the wave length of the laser.

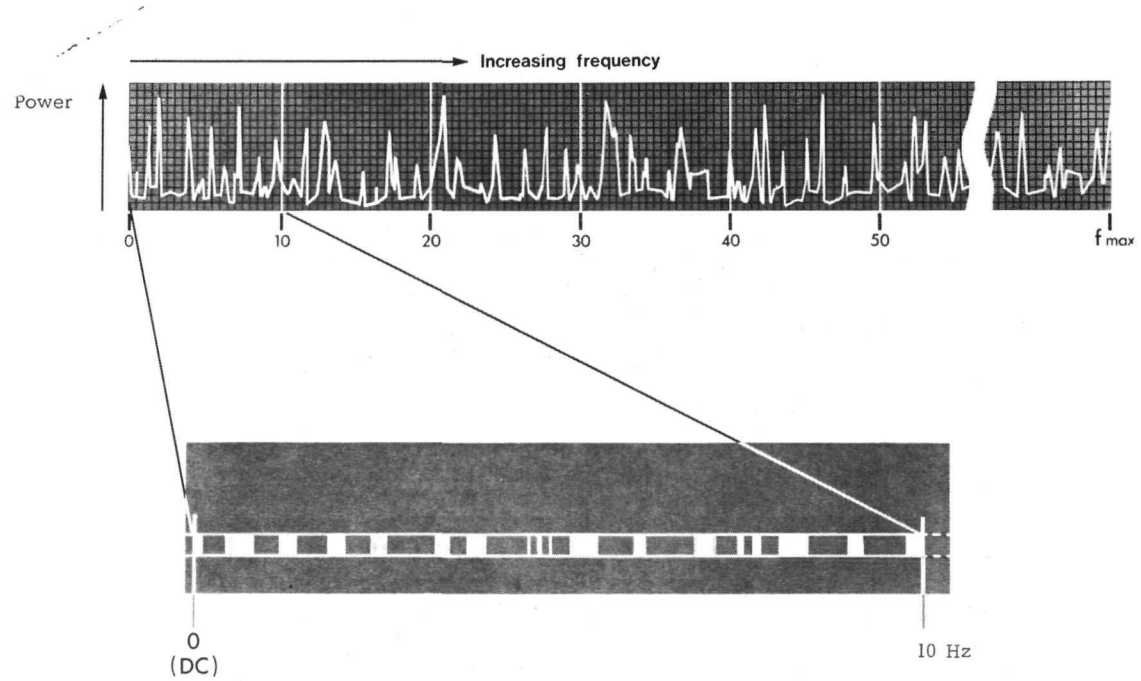

Fig. 1.9 Light Intensity is Proportional to Signal Power

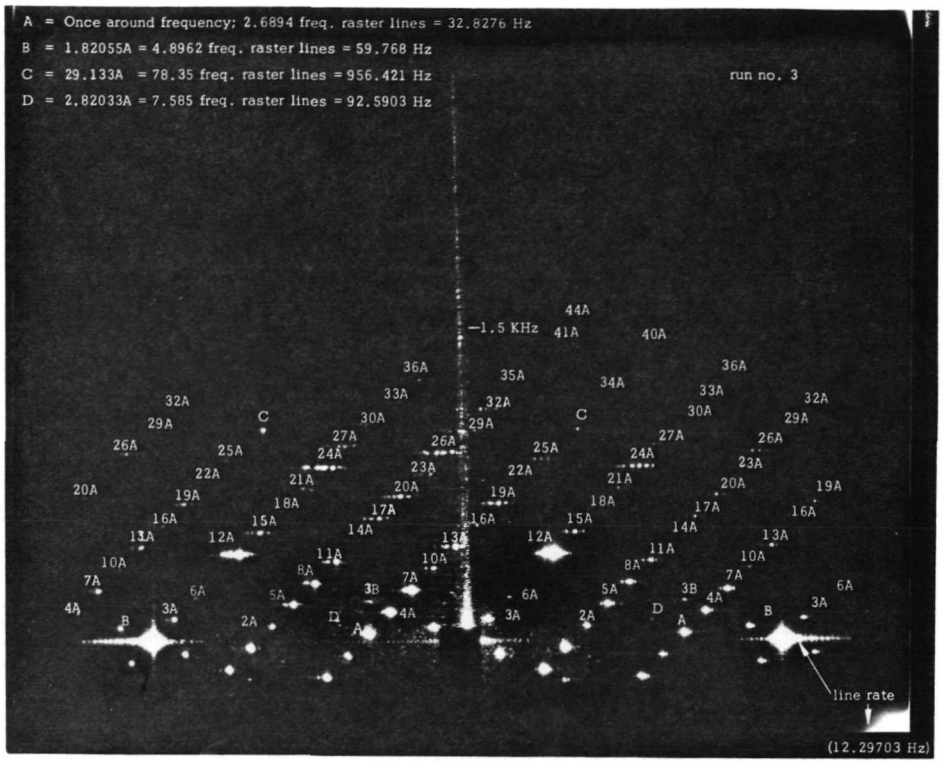

Fig. 1.10 Frequency Plane Spectrum of a Reciprocating Air Compressor

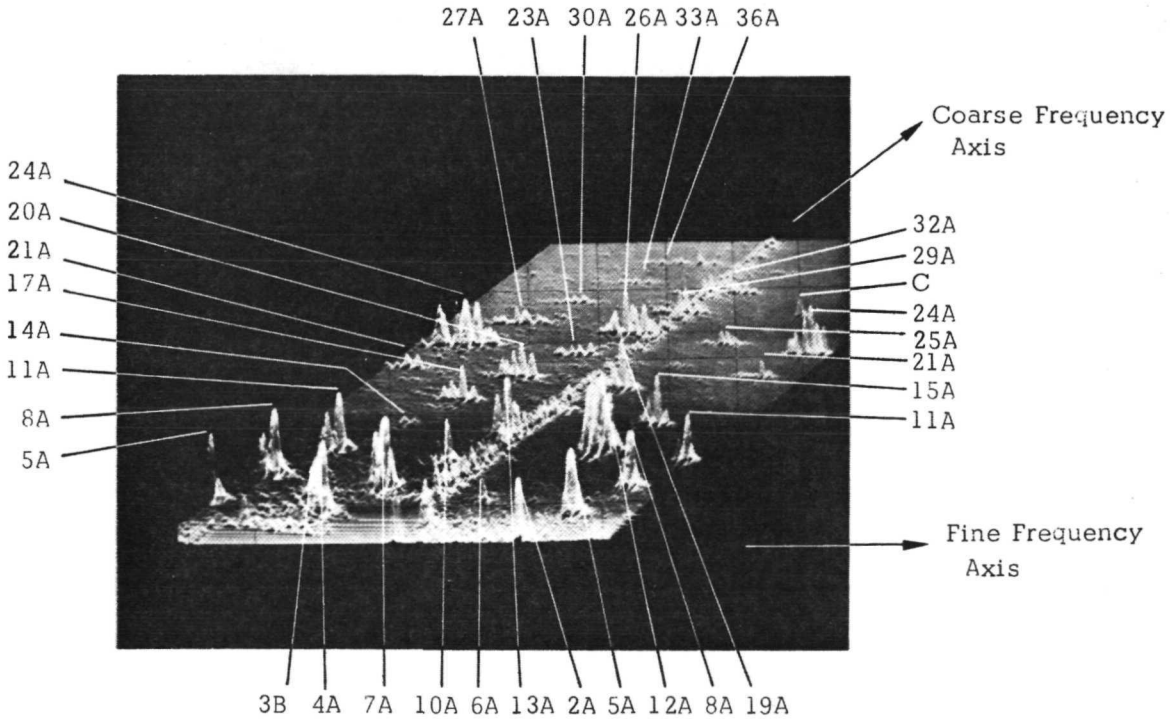

A = Once around frequency of air compressor

Fig. 1.11 Isometric of Air Compressor Spectrum

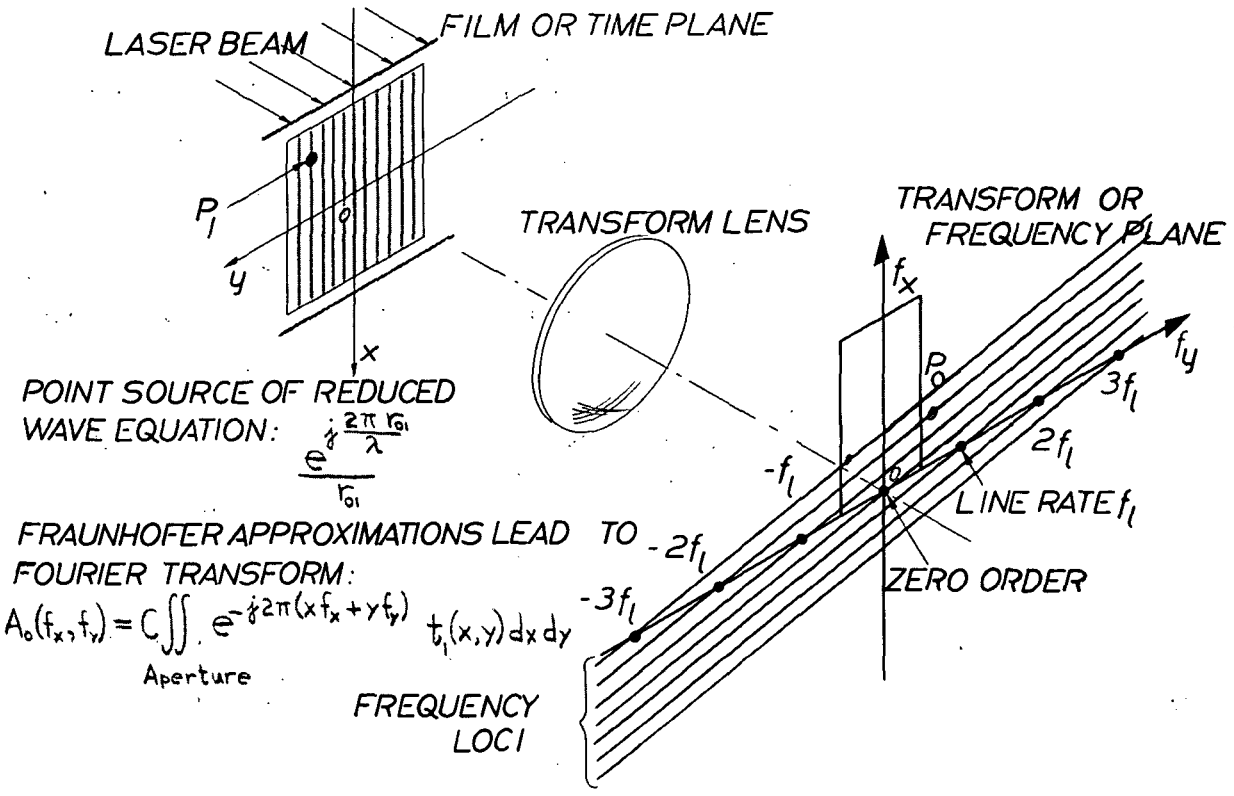

Fig. 1.12 Formation of Fourier Transform

About a century and a half ago, Franuhofer showed that when the observation or frequency plane is far from the film plane, then the essential variable part of r_{01} only depends upon the sum of products of correspondingly directed coordinates in the two planes, cf. Goodman*. The resulting simple form for the amplitude of light A_o at observation point P_o is given by the integral at the bottom of the figure. The exponential has been simplified so that, by superposition, A_o is directly proportional to the Fourier transform of the transmittance t_1 extended over the entire uniformly illuminated aperture. The introduction of the transform lens preserves the relation and allows the two planes to be brought conveniently close together.

By further calculations, it can be shown that the Fourier transform of the modulated raster scan recording has the following properties:

*Goodman, J. W., Introduction to Fourier Optics, McGraw-Hill, New York, 1968.

1. The presence of any coherent component in the recording will produce a bright spot in the frequency plane.
2. That spot must lie on one of the frequency loci which form another raster indicated by the inclined parallel lines passing through the line rate spot and its harmonics.
3. Each spot is repeated periodically in the f_y direction with period f_ℓ.
4. In a manner similar to that of the time raster in the film plane, motion along a locus corresponds to a continuous variation of frequency, but motion in the positive f_x direction to the next locus corresponds to an increase in frequency by exactly the line rate f_ℓ.

Because of the periodicity in the frequency plane, the entire spectrum is displayed in any vertical strip of width f_ℓ. It is convenient to use the shaded strip of Fig. 1.12 bounded on the left by the f_x - axis, below by the f_y - axis, and on the right by the vertical line $f_y = f_\ell$. That strip corresponds to the raster display of Fig. 1.8. However, in some instances we prefer to use the symmetrically located strip, indicated by solid lines, which is bounded on the left and right by $f_y = -f_\ell/2$ and $f_y = +f_\ell/2$ respectively.